Quantification of Retinal Tissue Damage

Semester Long Research Project Report

Raghav Singh
Sanjeev Dubey
Utkarsh Mittal

Under the guidance of

Dr. Nirmal Yadav
Associate Professor, Cluster Innovation Centre

May 2017

Acknowledgement

We would like to acknowledge with thanks and appreciation all the people who played a role in the successful completion of this project.

Our sincere thanks go to our mentor, Dr. Nirmal Yadav, who guided us throughout the stages of this project. Finally, we would also like to thank Cluster Innovation Center for providing us with the facilities and the necessary resources to complete our work.

Certificate

This is to certify that the present work embodied in this report entitled "**Quantification of Retinal Tissue Damage**" has been submitted to the Cluster Innovation Centre, University of Delhi towards the partial fulfillment of the Semester Long Research Project. This project has not been submitted in part or full to any other University/Institution for the award of any other degree or diploma. The work has been carried out at the Cluster Innovation Centre, University of Delhi under the supervision of Dr. Nirmal Yadav. However, the supervisor does not undertake any responsibility of authenticity of text.

.

Dr. Nirmal Yadav

(Mentor)

Raghav Singh
Sanjeev Dubey
Utkarsh Mittal

(Candidate)

Contents

List of Figures

List of Tables

Abstract

Retina is the outer lining of human eye where the image formation takes place. Any threat to retina causes severe eye defects and may lead to complete blindness. During a defect the retina gets distorted. To measure the severity of a disease we need to determine different retinal tissue damages. These damages must be quantified to make useful predictions. Here we attempt to quantify retinal tissue damage through various image processing techniques. To verify our estimate we applied machine learning algorithms to create a classifier for detection of diabetic retinopathy and macular edema disease.

Diabetic retinopathy & Macular Edema are diseases prone to diabetic people. They cause progressive damage to the retina of the eye. DR is the leading cause of blindness in the working-age population of the developed world. It is estimated to affect over 93 million people.

1. Introduction

To study retina a retinal examination is done. The images of retina are taken through either fundus photography or Optical coherence Tomography (OCT). OCT is a recent advancement in medical imaging. OCT data is 3-D profile consisting of different layers of retina. There are works on OCT data which focuses on determining the change in thickness of different retinal layers. Fundus photography involves capturing a photograph of the back of the eye. Specialized fundus cameras that consist of a microscope attached to a flash enabled camera are used in fundus photography. Fundus images are then analyzed by ophthalmologists who look for certain patterns and defects in the image to predict diseases. There are many problems in this system. World is short of highly qualified ophthalmologists. Due to this people have to wait for long before starting medications. This sometimes worsens the condition. Another crucial disadvantage is lack of agreement between different doctors on a single profile of fundus.

We have started with fundus images to analyze retina. Our project aims to analyze these defects through sophisticated image processing techniques. Based on known patterns and defects we extract features from fundus image. These features are taken and put into a classifier. The classifier comes out with a decision based on its learning.

Diabetic Retinopathy is an active research area. A lot of research has been done in last few years. Computer scientists and medical researchers have developed many algorithms for automatic detection of eye diseases, though accuracy has never been very great. Researchers have been trying new features and new algorithms to improve further. Joshi, Karule[1] have used morphological operations for image segmentation. Hussain et al.[2] have local variation operators and split and merge algorithm to detect fine exudates. Shraddha et al.[3] detected exudates by calculating differential morphological profile (DMP). This approach has very good specificity and PPV values as 99.99% and 98.23% respectively.

In this report we have put our work in three different sections. First we have thoroughly explained all the major concepts over which we have built our work. In next section we have described the feature extraction procedures for blood vessels, microaneurysms, exudates and haemorrhages. In the last section the data generated from these features has been visualised. Finally we have put the results and concluded our work.

1.1 Radon Transformation:

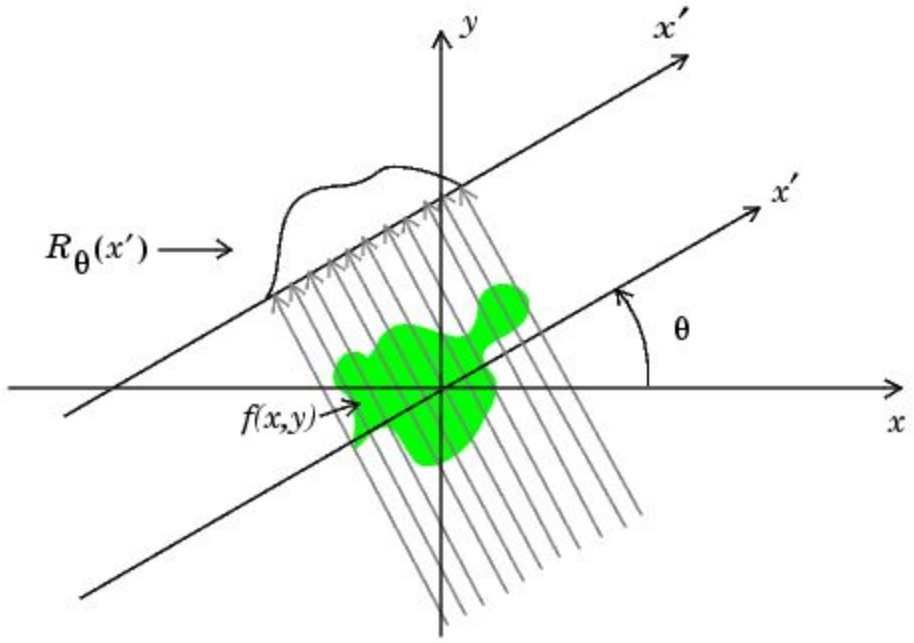

Figure 1: Radon transform for a point R-theta(x')

The Radon transform is an integral transform whose inverse is used to reconstruct images from medical CT scans. As given in the figure, we measure the projections as an integral of f along the z axis for every r. The orientation of the (r,z) coordinate axes relative to the x,y axes. The z axis is parallel to the direction of X-rays. For this analysis, we assume that the source and detectors employ parallel beam geometry. For a given $\theta \in$ [0, 180°), the X-rays are θ degrees counterclockwise from the y axis. The line integral along z is measured for every $r$at the given θ.

Since the image is only available to us as a function of x and y, we rotate the (x,y) coordinates to express them in terms of r and z. Also note that theoretically, projections are only required for $\theta \in$ [0, 180°). It does not matter which direction we integrate from along the z-axis.

1.2 OCT Image Analysis:

OCT uses low-coherence interferometry to produce a two-dimensional image of optical scattering from internal tissue microstructures. OCT has longitudinal and lateral spatial resolutions of a few micrometers and can detect reflected signals as small as ~10 of the incident optical power. Over the 15 years since the original description, optical coherence tomography (OCT) has become one of the key diagnostic technologies in the ophthalmic subspecialty areas of retinal diseases and glaucoma. The reason for the widespread adoption of this technology originates from at least two properties of the OCT results: on one hand, the results are accessible to the non-specialist where microscopic retinal abnormalities are grossly and easily noticeable; on the other hand, results are reproducible and exceedingly quantitative in the hands of the specialist.

Working:

OCT is based on imaging of reflected light. But unlike a simple camera image that only has transverse dimensions(left/right, up/down) it revolves depth. The depth resolution us of the order 0.01 mm or 0.4 thousandth of an inch. This provides cross-sectional views (tomography) of internal tissue structures similar to tissue sections under a microscope. Thus, OCT has been.described as a method for non-invasive tissue 'biopsy'.With this technique it is possible to perform noninvasive cross-sectional imaging of internal structures in biological tissues by measuring their optical reflections.

OCT has been used to measure volume and total thickness of the retina along with structural changes of the various cellular layers of the retina with the aid of segmentation algorithms. The role of OCT in the assessment and management of retinal diseases has become significant in understanding the vitreoretinal relationships and the internal architecture of the retinal structure.OCT has also improved diagnosis and management of retinal diseases by reducing reliance on insensitive tests such as perimetry and subjective disc grading. Thickness differences characterizes regions with early pathological signs from normal regions and differences in optical properties and texture descriptors of normal and abnormal retinal tissue may also provide additional information of disease development in pathological eyes. The appropriateness of texture to classify tissues in OCT images has been shown in previous studies.

A potential improvement in the clinical application of OCT to eye diseases is the quantification of the anatomic changes along with the dysfunction of the cellular layers of the neurosensory retina. Our preliminary results suggest that the fractal dimension of the intraretinal layers might provide useful information to differentiate MDR eyes, which are characterized by

neurodegeneration at the early stages, from healthy eyes in addition to the structural information

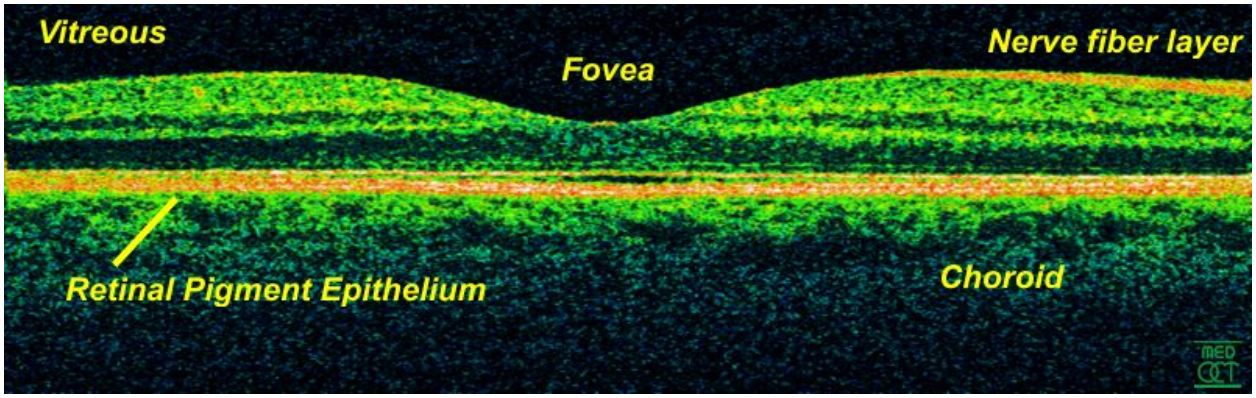

Figure 2: An OCT cross-sectional image.

A potential improvement in the clinical application of OCT to eye diseases is the quantification of the anatomic changes along with the dysfunction of the cellular layers of the neurosensory retina. Our preliminary results suggest that the fractal dimension of the intraretinal layers might provide useful information to differentiate MDR eyes, which are characterized by neurodegeneration at the early stages, from healthy eyes. Fractal analysis provided a better sensitivity, offering a potential diagnostic predictor for detecting early neurodegeneration in the retina. In this study, we evaluated the diagnostic power of a novel method based on the fractal analysis of OCT derived retinal tissue layer properties in discriminating normal healthy eyes from diabetic eyes with early neural loss. Although texture measures of the retinal tissue are not standardized measures for detecting significant intraretinal changes, texture-based measures were obtained from OCT intensity images and used in the fractal dimension analysis. In addition, the fractal analysis' diagnostic outcome was compared with the standard approach that uses structural information extracted from OCT images. Specifically, we calculated fractal dimension and thickness using features measured locally for each intraretinal layer and evaluated their suitability to quantify retinal tissue damage.

A method based on the power spectrum was used to calculate the fractal dimension in OCT images . Since the average power spectrum of an image obeys a power law scaling, the fractal dimension was calculated from the power law detected in the graph of the power spectrum as a function of the frequency in the Fourier transform of the OCT image (gray scale). In this particular case, when the graph is plotted in a log-log scale the curve is approximately similar to a straight line and the dimension is provided by the slope of the line. The fast Fourier transform (FFT) was applied to the OCT reflectivity profiles to obtain the power spectrum.

$$\mathbf{FD = (5-B)/2}$$

The mean value of the fractal dimension was calculated by averaging the fractal dimension measurements across all A-scans in each macular region of each intraretinal layer.

A potential improvement in the clinical application of OCT to eye diseases is the quantification of the anatomic changes along with the dysfunction of the cellular layers of the neurosensory retina. Our preliminary results suggest that the fractal dimension of the intraretinal layers might provide useful information to differentiate MDR eyes, which are characterized by neurodegeneration at the early stages, from healthy eyes in addition to the structural information.

1.3 Fractal Dimension:

Fractals are self-similar structures at every scale. As mathematical equations, fractals are usually nowhere differentiable. The mathematical roots of the idea of fractals have been traced throughout the years as a formal path of published works, starting in the 17th century with notions of recursion, then moving through increasingly rigorous mathematical treatment of the concept to the study of continuous but not differentiable functions in the 19th century by the seminal work of Bernard Bolzano, Bernhard Riemann, and Karl Weierstrass, and on to the coining of the word fractal in the 20th century with a subsequent burgeoning of interest in fractals and computer-based modelling in the 20th century. The term "fractal" was first used by mathematician Benoît Mandelbrot in 1975. Mandelbrot based it on the Latin frāctus meaning "broken" or "fractured", and used it to extend the concept of theoretical fractional dimensions to geometric patterns in nature.

There is some disagreement amongst authorities about how the concept of a fractal should be formally defined. Mandelbrot himself summarized it as "beautiful, damn hard, increasingly useful. That's fractals."

We consider N=r^D, take the log of both sides, and get log(N) = D log(r). If we solve for D. D = log(N)/log(r). This generalized treatment of dimension is named after the German mathematician, Felix Hausdorff. It has proved useful for describing natural objects and for evaluating trajectories of dynamic systems.

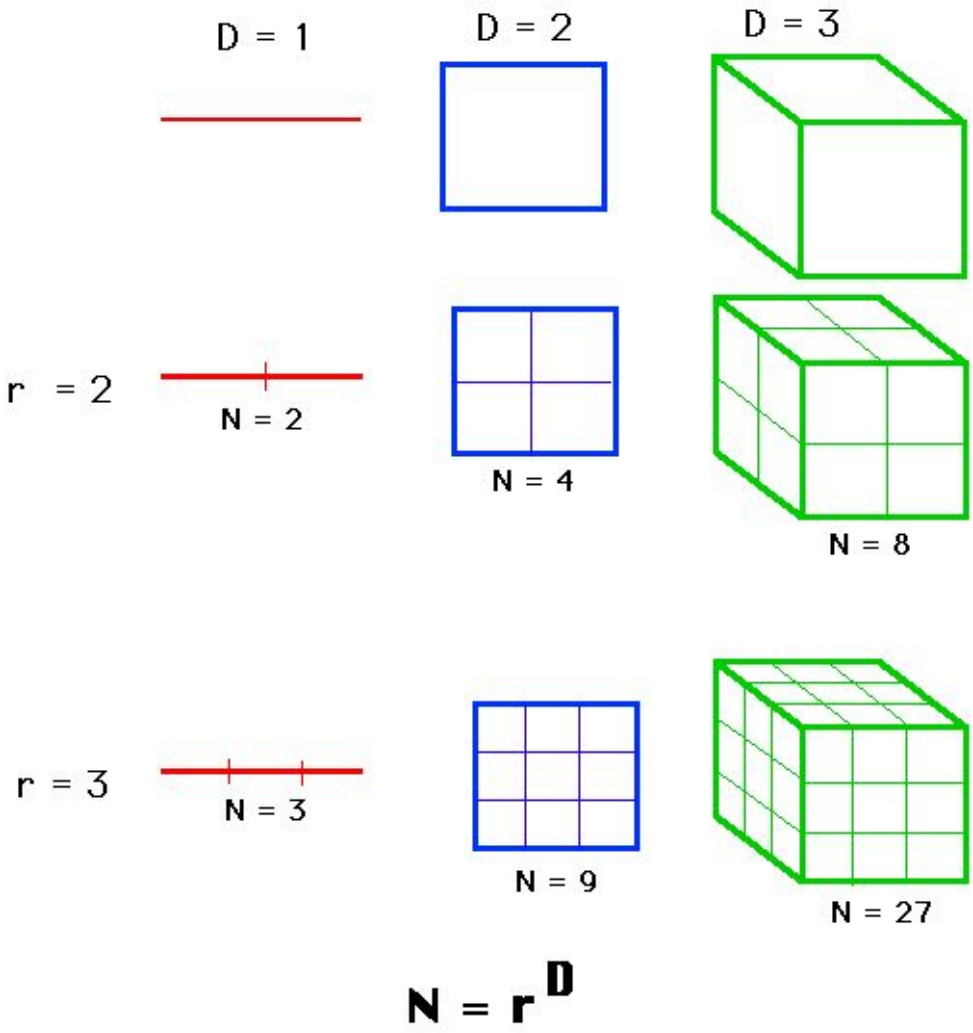

Figure 3: Fractal Dimension for n = 1,2 and 3

Box Counting Method:

Consider a square, if we subdivide it into smaller squares each with 1/2 the side length then it takes 4 of these smaller pieces to form the original square. If we subdivide the square into smaller squares each with 1/4 of the side length then it takes 16 of them to form the original square. As above we can write an expression for the number of pieces we need of size "s" to cover the original square, it is $N(s) = (1/s)^2$.

Repeat for a cube....$N(s) = (1/s)^3$.

The exponents 1, 2, and 3 in the above examples are fundamental to our concept of the dimension involved. This can be generalised to $N(s) = (1/s)^D$ where D is the dimension, an

integer as above but it need not be. If we take logarithms of both sides we have log(N(s)) = D log(1/s), in order words we can estimate the dimension by plotting log(N(s)) against log(1/s) the slope of which is the dimension, if it isn't an integer then it's a fractional (fractal) dimension.

1.4 Methodology

Methodology of the project can be overseen as follows:

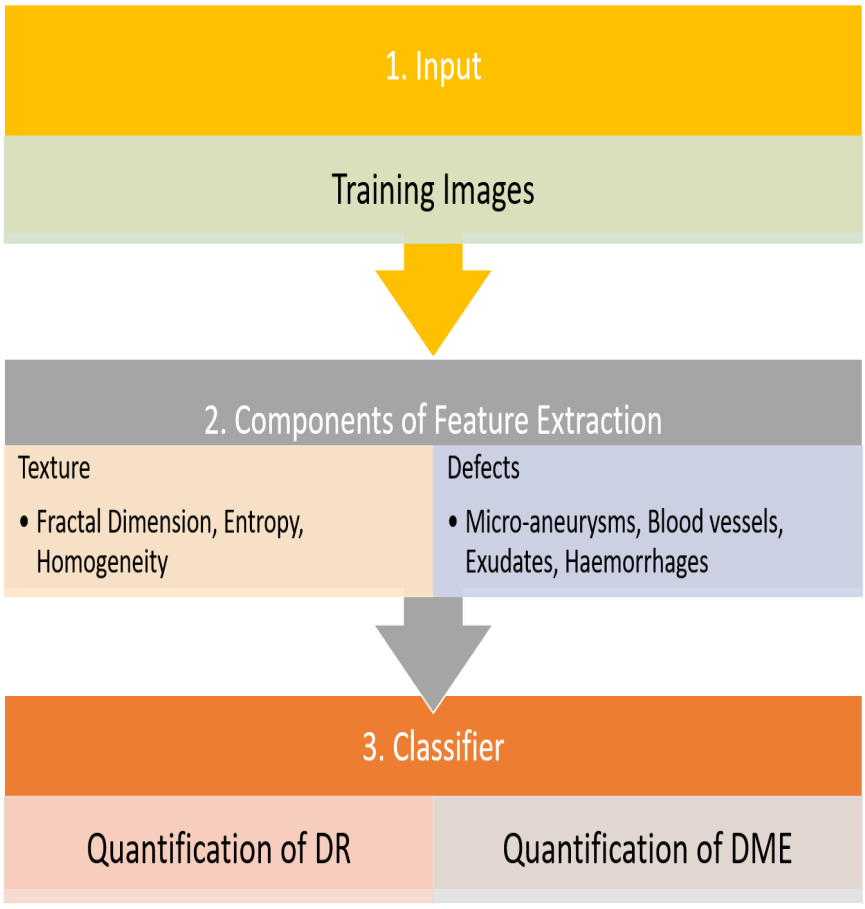

2. Study of FUNDUS images

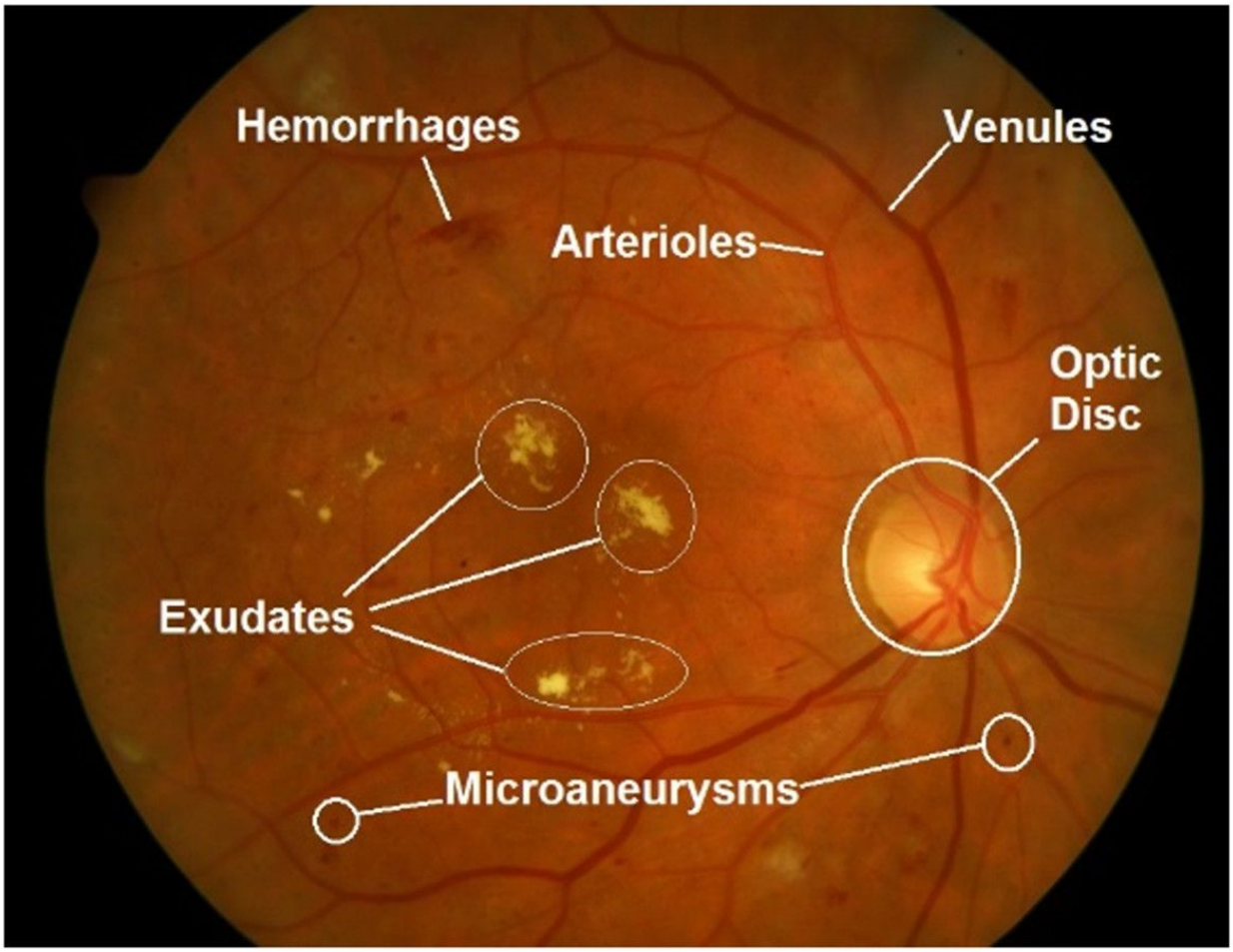

Figure 4: A labelled fundus image depicting features of retina.

The Ministry of Health estimates that 69 crore people in india have diabetes and the World Health Organization estimates that 34.7 crore people have this disease in india.. Diabetic Retinopathy (DR) is an eye disease associated with long-standing diabetes. Around 40% to 45% Indians with diabetes have some stage of the disease. Diabetic Retinopathy is the leading cause of blindness in the working-age population of the developed world. It is estimated to affect over 93 million people. Progression to vision impairment can be slowed or averted if DR is

detected in time, however this can be difficult as the disease often shows few symptoms until it is too late to provide effective treatment.

Currently, detecting DR is a time-consuming and manual process that requires a trained clinician to examine and evaluate digital color fundus photographs of the retina. By the time human readers submit their reviews, often a day or two later, the delayed results lead to lost follow up, miscommunication, and delayed treatment. Also, india has a shortage of close to 1,27,000 ophthalmologists and lacks crucial eye health infrastructure and facilities.

Clinicians can identify DR by the presence of lesions associated with the vascular abnormalities caused by the disease. While this approach is effective, its resource demands are high. The expertise and equipment required are often lacking in areas where the rate of diabetes in local populations is high and DR detection is most needed. As the number of individuals with diabetes continues to grow, the infrastructure needed to prevent blindness due to DR will become even more insufficient.

The need for a comprehensive and automated method of DR screening has long been recognized, and previous efforts have made good progress using image classification, pattern recognition, and machine learning. Routine retinal screening for DR even at the time of diagnosis of type 2 diabetes may help in optimized laser therapy. Annual retinal examination and early detection of DR can considerably reduce the risk of visual loss in diabetic individuals. Developing CAD systems raised a progressive need of image processing tools that provide fast, reliable, and reproducible analysis of major anatomical structures in retinal Fundus images. **Segmentation of these retinal anatomical structures is the first step in any automatic retina analysis system.**

2.1 Steps of feature segmentation:

Retinal image segmentation includes several steps; morphological processing, thresholding, edge detection and adaptive histogram equalization. These steps will be explained in the following subsections.

I. **Morphological Processing:** Morphology is the study of shape. Mathematical morphology deals with the mathematical theory of describing shapes using sets. In image processing, Mathematical morphology is used to investigate the interaction between an image and a certain chosen structuring element using the basic operations of erosion and dilation.The main processes used here are dilation, erosion, opening, and closing .These processes involve a special mechanism of combining two sets of pixels. Usually, one set consists of the image being processed and the other constitutes the structuring element or kernel. Two very important transformations are opening and closing. Intuitively, dilation expands an image object and erosion shrinks it. An essential

part of the dilation and erosion operations is the structuring element (SE) used to probe the input image. A structuring element is a matrix consisting of only 0s and 1s that can have any arbitrary shape and size. Figure 2 shows diamond, disc, and octagon shaped structuring elements. Opening generally smoothes the contour in an image. Closing tends to narrow smooth sections of contours, eliminating small holes and filling gaps in contours. Algorithms combining the above processes are used to create mechanisms of edge detection, noise removal and background removal as well as for finding specific shapes in images. We will briefly review morphological operations used in this paper. Let f(x, y) a finite-support grayscale image function defined on grid Z2 and B be a binary structuring element.

Opening: $f \bigcirc B = (f \ominus B) \oplus (B)$. (1)

Closing: $f \bullet B = (f \oplus B) \ominus (B)$. (2)

Dilation : $(f \oplus B)(x, y) = \max\{f(x - s, y - t) | (s, t) \in B\}$. (3)

Erosion: $(f \ominus B)(x, y) = \min\{f(x+s, y+t) | (s, t \in B\}$. (4)

In practical image processing, it is sufficient to know that morphology can be applied to a finite set P if

1. We can partially order its elements.

2. Each non-empty subset of P has a maximum and minimum.

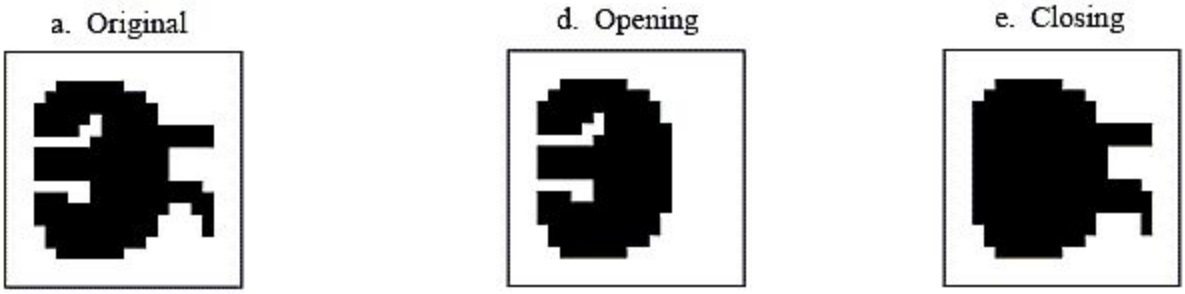

Figure 5: Image showing morphological operations opening and closing on original image

II. **Thresholding:** Thresholding is useful to remove unnecessary details from an image to concentrate on essentials. In the case of Fundus images, by removing all gray level information, the blood vessels are reduced to binary pixels. It is necessary to distinguish blood vessels foreground from the background information. Thresholding can also be used to bring out hidden details. It is very useful in the image region, which is obscured by similar gray levels. Therefore, choosing an appropriate threshold value is important,

because a low value may decrease the size of some of the objects or reduce the number of these objects and a high value may include extra background information.

Thresholding helps us in converting image's features into numerical data which is then applied on various machine learning algorithms as finding binary values in images is easy. This provides as a channel to convert fundus images into numerical values. There are various thresholding algorithms such as OTSU, adaptive, etc.

III. **Edge Detection:** Canny method is used for edge detection. The Canny method performs better than the other edge detection methods, because it uses two thresholds to detect strong and weak edges, and for this reason, Canny algorithm is chosen for edge detection in the proposed technique.

Canny edge detection is a technique to extract useful structural information from different vision objects and dramatically reduce the amount of data to be processed. It has been widely applied in various computer vision systems. Canny has found that the requirements for the application of edge detection on diverse vision systems are relatively similar. Thus, an edge detection solution to address these requirements can be implemented in a wide range of situations. The general criteria for edge detection includes:

1. Detection of edge with low error rate, which means that the detection should accurately catch as many edges shown in the image as possible.
2. The edge point detected from the operator should accurately localize on the center of the edge.
3. A given edge in the image should only be marked once, and where possible, image noise should not create false edges.

The Process of Canny edge detection algorithm can be broken down to 5 different steps:

1. Apply Gaussian filter to smooth the image in order to remove the noise.
2. Find the intensity gradients of the image.
3. Apply non-maximum suppression to get rid of spurious response to edge detection.
4. Apply double threshold to determine potential edges.
5. Track edge by hysteresis: Finalize the detection of edges by suppressing all the other edges that are weak and not connected to strong edges.

IV. **Adaptive Histogram Equalization:**

Histogram equalization usually increases the global contrast of many images, especially when the usable data of the image is represented by close contrast values. Through this adjustment, the intensities can be better distributed on the histogram. This allows for areas of lower local contrast to gain a higher contrast. Histogram equalization accomplishes this by effectively spreading out the most frequent intensity values. A disadvantage of the method is that it is

indiscriminate. It may increase the contrast of background noise, while decreasing the usable signal.

Adaptive histogram equalization (AHE) is a computer image processing technique used to improve contrast in images locally. It differs from ordinary histogram equalization in the respect that the adaptive method computes several histograms, each corresponding to a distinct section of the image, and uses them to redistribute the lightness values of the image. It is therefore suitable for improving the local contrast and enhancing the definitions of edges in each region of an image.

While performing AHE if the region being processed has a relatively small intensity range then the noise in that region gets more enhanced. It can also cause some kind of artifacts to appear on those regions. To limit the appearance of such artifacts and noise, a modification of AHE called CLAHE can be used. The amount of contrast enhancement for some intensity is directly proportional to the slope of the CDF function at that intensity level. Hence contrast enhancement can be limited by limiting the slope of the CDF. The slope of CDF at a bin location is determined by the height of the histogram for that bin. Therefore if we limit the height of the histogram to a certain level we can limit the slope of the CDF and hence the amount of contrast enhancement.

The only difference between regular AHE and CLAHE is that there is one extra step to clip the histogram before the computation of its CDF as the mapping function is performed.

Following is the overview of the algorithm for this function:

1. Calculate a grid size based on the maximum dimension of the image. The minimum grid size is 32 pixels square.
2. If a window size is not specified chose the grid size as the default window size.
3. Identify grid points on the image, starting from top-left corner. Each grid point is separated by grid size pixels.
4. For each grid point calculate the histogram of the region around it, having area equal to window size and centered at the grid point.
5. If a clipping level is specified clip the histogram computed above to that level and then use the new histogram to calculate the CDF.
6. After calculating the mappings for each grid point, repeat steps 6 to 8 for each pixel in the input image.
7. For each pixel find the four closest neighboring grid points that surround that pixel.
8. Using the intensity value of the pixel as an index, find its mapping at the four grid points based on their cdfs.
9. Interpolate among these values to get the mapping at the current pixel location. Map this intensity to the range [min:max) and put it in the output image.

Clipping the histogram itself is not quite straight forward because the excess after clipping has to be redistributed among the other bins, which might increase the level of the clipped histogram. Hence the clipping should be performed at a level lower than the specified clip level so that after redistribution the maximum histogram level is equal to the clip level.The CLAHE algorithm partitions the images into contextual regions and applies the histogram equalization to each one. This evens out the distribution of used grey values and thus makes hidden features of the image more visible.

2.2 Features of Fundus Images:

A. Detection of Blood Vessels:

Blood vessels are very important features which help in examination of retina. Blood vessels show different symptoms when an eye suffers from certain disease. There are swellings in the blood vessel when an eye has diabetic retinopathy. In non proliferative diabetic retinopathy the narrow blood vessels do not get enough blood supply because of blockage near optic nerve. It causes them to get broken down and release fluid in the retina. In the proliferative retinopathy this gets worse. To counteract it, retina tries to develop new blood vessels. Again these blood vessels are weak and disoriented which sometimes causes them to leak inside vitreous.

So detection of blood vessels becomes very important. We have used Alternate sequential Filtering (ASF) along with other image processing techniques to extract blood vessels. We also tried to work on red channel of image and get it segmented. But the presence of haemorrhages and clots made it difficult. In our procedure we have extracted green channel of image because it has greater contrast. To further increase contrast we apply Contrast Limited Adaptive Histogram Equalization. Applying ASF on this image gives us another image with average intensity of each region applied over it. Later we subtract this image from output of CLAHE. This gives us an image which contains faint traces of blood vessels with optic disk and other things removed.

We binarize this image with a threshold T and get blood vessels segmented. The final image also contains noise and some undesirable elements. Noise is removed by eroding the image. Undesirable elements are removed by taking into account the feature that only blood vessels are linear in shape.

(a) (b) (c)

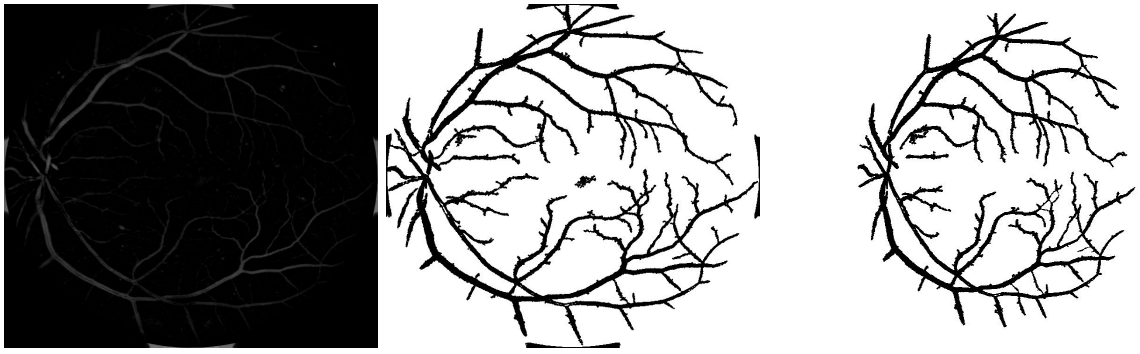

(d) (e) (f)

Figure 6: Various steps in blood vessel segmentation

(a) : Input image of fundus

(b) : Output of CLAHE on green channel

(c) : Alternate Sequential Filtering of (b)

(d) : Subtraction result of (b) and (c)

(e) : Thresholded image with noise and extra elements

(f) : Segmented blood vessels

B. Detection of Haemorrhages:

Haemorrhages are chunks of blood vessels lying on the retina because of leakage. Presence of Haemorrhages are a good indicator of retinal damage. In a fundus image haemorrhages appear as red blobs. In proliferative diabetic retinopathy we see small as well as some very large traces of haemorrhages.

To detect haemorrhages we followed the same procedure as we did in blood vessel detection upto some steps. When we get the image (f) we do xor operation on current image and image obtained after segmenting blood vessels. This gives us an image which contains haemorrhages and small noise elements. To remove noise we apply a median filter on image. The new image has haemorrhages but also some small and broken blood vessels. To remove them we take all the contours and check if it can be approximated as a polygon of side greater than 5. Those which pass certainly have a non linear shape (i.e. complex circular) and are counted as haemorrhages.

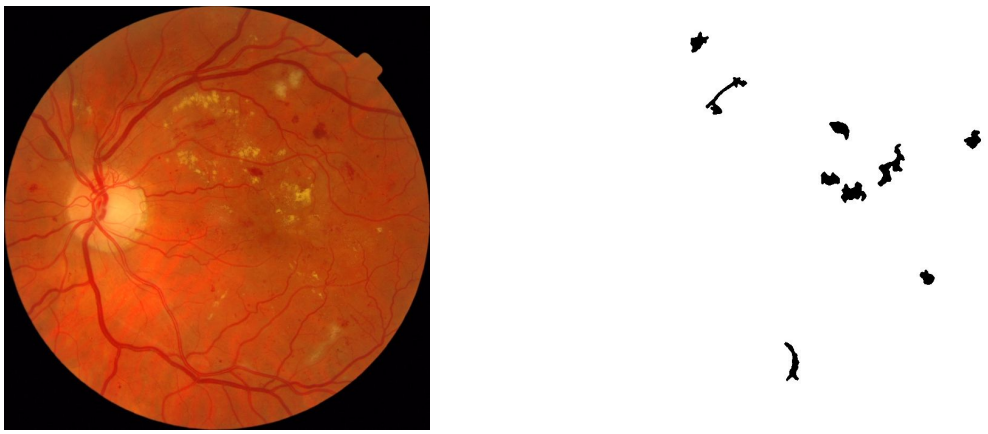

Figure 7: Fundus image(L) and its haemorrhages (R)

C. Detection of Exudates:

Exudates are another important feature of retinal analysis. Exudates are bulges of yellow and white colors appearing in the fundus. There are two types of exudates namely hard and soft exudates. Hard exudates consist of extracellular lipid which has leaked from abnormal retinal capillaries. Hard exudates are found principally in the macular region and as the lipids coalesce and extend into the central macula (fovea), vision can be severely compromised. Soft exudates looking like cotton wool, are nerve fiber layer infarcts.

Exudates have been detected using red and blue channel. We know that yellow color consists majorly of red and green color. We thresholded the red channel and green channel individually taking threshold T as (max(channel)+mean(channel))/2. These two binary channels were passed through AND gate which gives us all the yellow coloured pixels. Now in the image we have exudates along with optic disk. To remove optic disk we have devices an algorithm.

We make a window of suitable size which scans the image with a stride s. For every scan we calculate the mean intensity of every window. Since optic disk is bigger in size and has very high intensity, we get the maximum at optic disk. To remove it we mask it with a window of black color. Thus we get only exudates in our image.

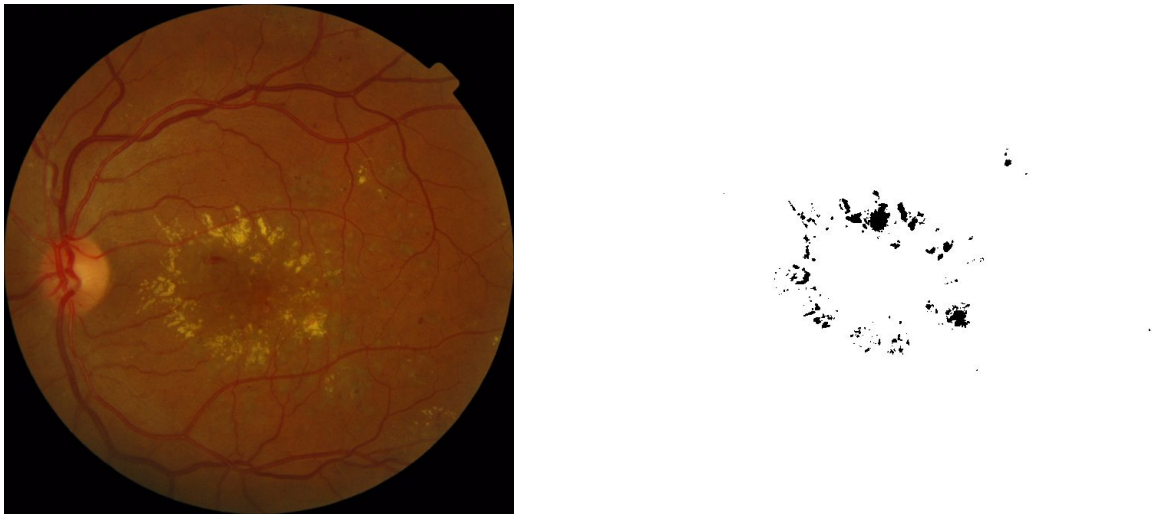

Figure 8: Fundus and its segmented exudates

D. Calculation of Fractal Dimension:

Fractal dimension is measured as a feature to quantify for texture of retina. Consider a line, if we subdivide the line in half then it takes two bits to recreate the original line. If we subdivide the line into 4 pieces it takes 4 of them to cover the line. We can write this generally, if we have a line segment of length "s' then the number of segments that will cover the original line is given by $N(s) = (1/s)^1$.

We have extracted Hausdorff fractal dimension using this algorithm:

- Pad the image with background pixels so that its dimensions are power of 2.

- Set the box size 'e' to the size of the image.

- Compute N(e), which corresponds to the number of boxes of size 'e' which contains at least one object pixel.

- If e > 1 then e = e / 2 and repeat previous step.

- Compute the points log(N(e)) x log(1/e) and use the least square method to fit a line to the points.

- The returned Hausdorff fractal dimension D is the slope of the line.

This gives us fractal dimension for fundus images which quantifies texture of retina.

E. Calculation of Homogeneity:

Homogeneity is another feature that is used to examine the texture of the retinal image which is calculated using the Gray-Level Co-Occurrence Matrix (GLCM). GLCM is a statistical method of examining texture that considers the spatial relationship of pixels. It is created by calculating how often pairs of pixel with specific values and in a specified spatial relationship occur in an image. Several statistics can be derived from this matrix which provide information about the texture of an image. Homogeneity is one such statistic that measures the closeness of the distribution of elements in the GLCM to the GLCM diagonal. Homogeneity weights values by the inverse of the contrast weight, with weights decreasing exponentially away from the diagonal as shown in the following equation. The addition of value '1' in the denominator is to prevent the value '0' during division. As homogeneity increases, the contrast typically decreases.

$$H = \sum_i \sum_j \frac{1}{1+(i-j)^2} p_d(i,j)$$

Where p_d is the probability of having a pair of pixel values (i,j) occurring in each image and (i,j) denotes a possible pair of the horizontally adjacent pixels i and j.

F. Calculation of Entropy:

Entropy is a statistical measure of randomness that can be used to characterize the texture of the input image. If image has more than two dimensions, the entropy function treats it as a multidimensional grayscale image and not as an RGB image. Entropy is defined as:

$$E = -\sum_i \sum_j (p * log_2 p)$$

where p is histogram values of gray scale image at different (i, j).

Entropy is a concept which originally arose from the study of the physics of heat engines. It can be described as a measure of the amount of disorder in a system. An organized structure, such as a crystal or a living organism, is very highly ordered and consequently has low entropy. When the crystal is heated sufficiently, it melts and becomes liquid, a much less ordered state. When the organism dies, it decays and becomes completely disrupted. In either system, its entropy increases. Another way of expressing entropy is to consider the spread of states which a system can adopt. A low entropy system occupies a small number of such states, while a high entropy system occupies a large number of states.

In the case of an image, these states correspond to the gray levels which the individual pixels can adopt. For example, in an 8-bit pixel there are 256 such states. If all such states are equally occupied, as they are in the case of an image which has been perfectly histogram equalized, the spread of states is a maximum, as is the entropy of the image. On the other hand, if the image has been thresholded, so that only two states are occupied, the entropy is low. If all of the pixels have the same value, the entropy of the image is zero. In this progression, as the entropy of the image is decreased, so is its information content. We moved from a full gray scale image, with high entropy, to a thresholded binary image, with low entropy, to a single-valued image, with zero entropy.

G. Detection of Microaneurysm:

Microaneurysm occur as small dark round dots (~ 15 - 60 mm) on fundus images. They are small bulges developed on weak blood vessels and are earliest sign of DR. The images are pre processed to a standard size of 1488 x 2240 and are of *.tif format.

The green channel of the image is extracted as it gives the best contrast between the microaneurysms and other bright parts such as optic disk, exudates, etc. Now, image contrast is further stretched by applying adaptive histogram equalization (CLAHE). The image contrast is stretched by applying adaptive histogram equalization before using edge detection (Canny method) to detect the outlines of the image. The boundary is detected by filling up the holes and a disc-shaped structuring element (SE) of radius 6 is created with morphological opening operation (erosion and dilation). The edge detection image is then subtracted from the image with boundaries to obtain an image without boundaries. After that, the holes or gaps are filled, resulting in microaneurysms and other unwanted artifacts. The blood vessels which are detected using the above mentioned method are subtracted from the image of microaneurysms and artifacts.

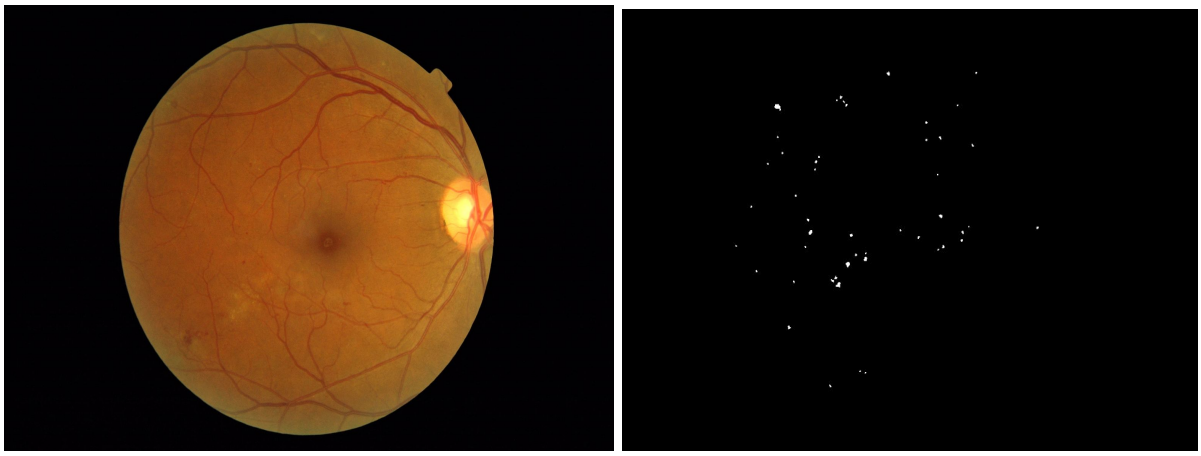

Figure 9: Fundus (L) and its segmented microaneurysm(R)

3. Data Analysis

To achieve our objective of quantification of retinal tissue damage, we have applied machine learning techniques to create a classifier for detection of diabetic retinopathy and macular edema disease.

3.1 Data Description

Features: As discussed earlier our features for the model proposed will contain earlier specified by image processing techniques and mathematical operations on the image. We combined these features with the already annotated labels. Our features were of two types:

***Retinal defects*:** Blood Vessel area, Microaneurysm area, Haemorrhage area

Structural features: Fractal Dimension, Entropy, Homogeneity

Data:

Our data comprises of numerical values of these 6 features. Converting images into numerical data is the first step in machine learning analysis. Now, the converted data was cleaned by l1 normalization and missing/ambiguous values were filled using median or mean for specific features like FD, etc.

Sample Data for 5 input data points:

imgname	dr	edema	entropy	hg	fd	bv	ma	haem
38557.tif	3	1	4.57	0.9805	1.3314	37318	2920	1935
43808.tif	0	0	4.29	0.99019	1.109	36651	33	766
43832.tif	1	0	4.11	0.9807	1.1464	38538	185	869
43882.tif	2	0	4.79	0.98332	1.618	48755	366	475
43906.tif	3	2	4.74	0.98428	1.5888	46405	443	2164

Table 1: Dataset made using features of fundus image.

3.2 Unimodal Distribution of Features:

The following graph shows the distribution of normalised features. Only ‘haemorrhage’ values are spread out, rest are all centered around and very close to zero.

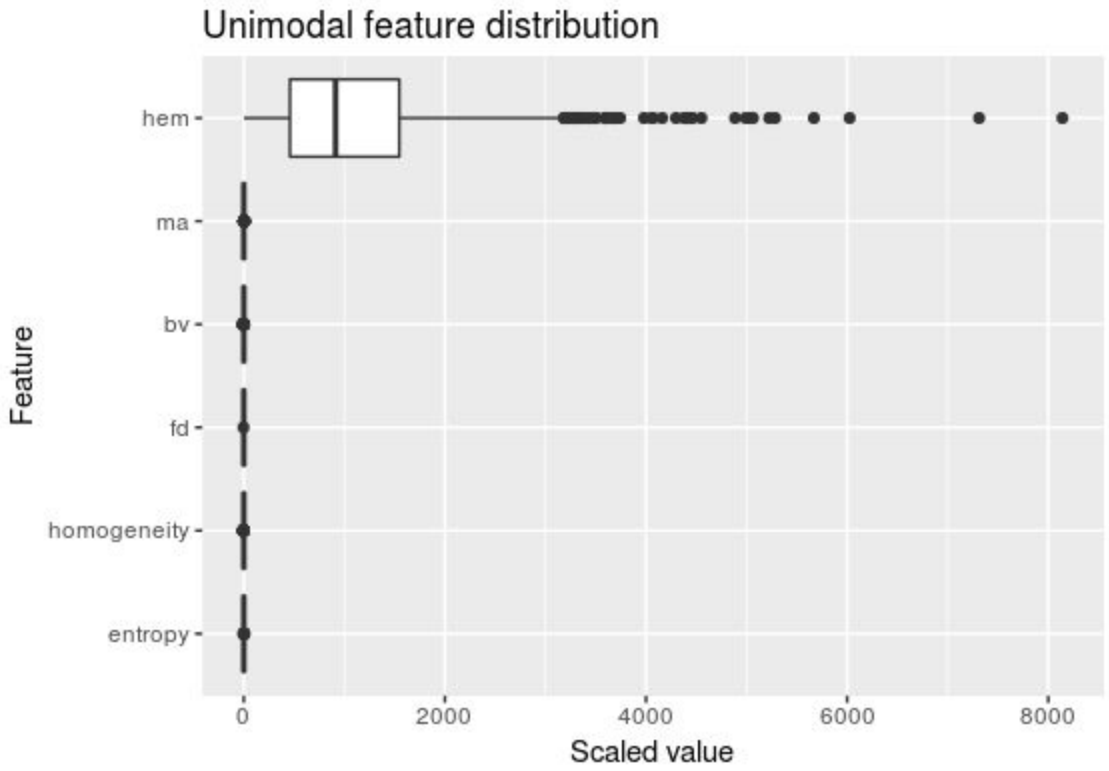

Figure 10: Unimodal feature distribution for machine learning

3.3 Correlation matrix:

The following figure shows the correlation matrix between all the features that are being taken into consideration. It is evident from the figure that entropy and fd share some positive correlation.

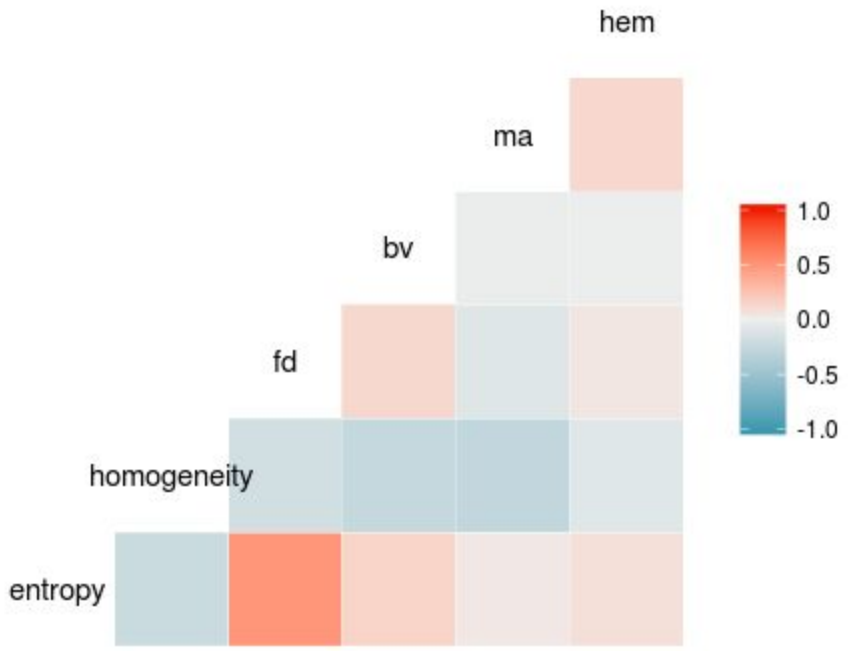

Figure 11: Depicts relation between two features at a time.

3.4 Scatter Plots for features:

The following figures show the scatter plots for all the features taken two at a time.

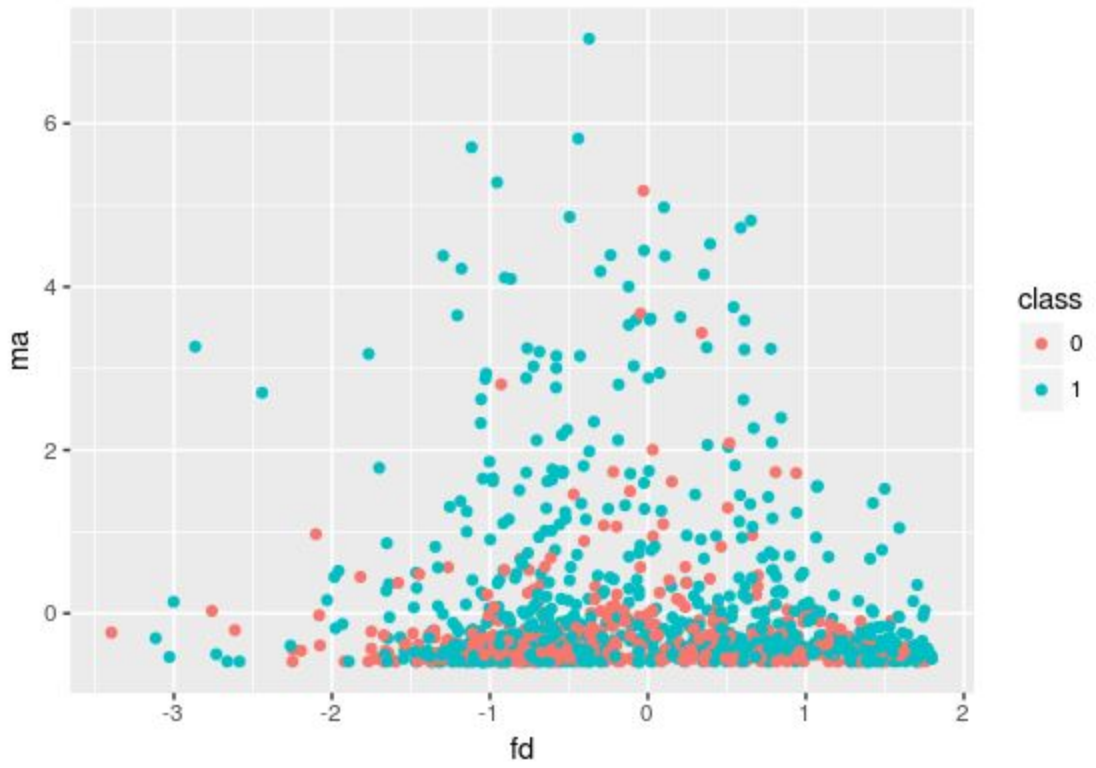

Figure 12: Scatter plots between two features at a time

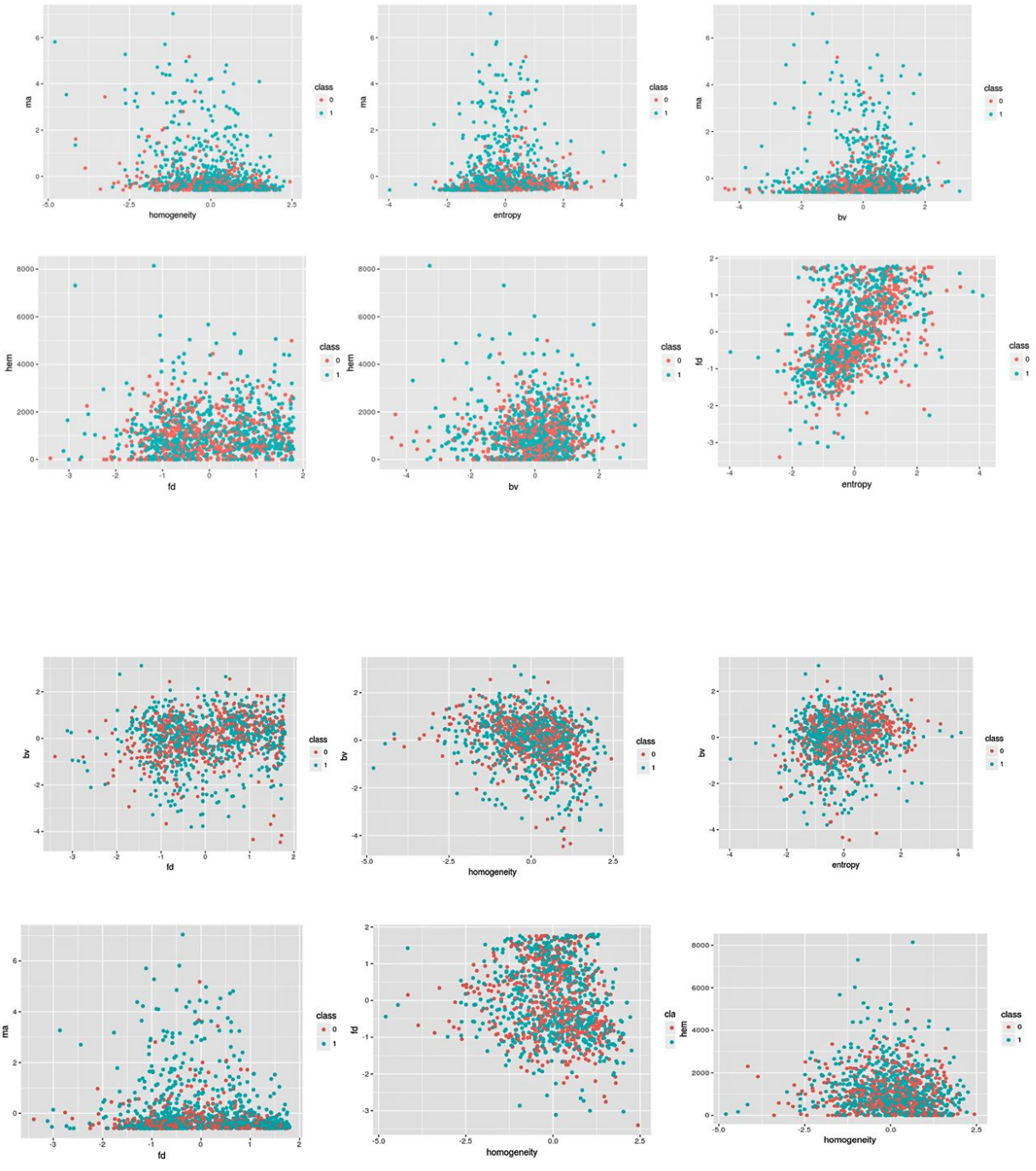
ma
homogeneity
entropy
bv
hem
fd
cla
class
0
1

***Principal Component Analysis*:** The main goal of a PCA analysis is to identify patterns in data; PCA aims to detect the correlation between variables. If a strong correlation between variables exists, the attempt to reduce the dimensionality only makes sense. In a nutshell, this is what PCA is all about: Finding the directions of maximum variance in high-dimensional data and project it onto a smaller dimensional subspace while retaining most of the information. PCA generates at most n number of features corresponding to number of features selected.

4. Results and Discussion

We fed our data into various Machine-Learning models and calculated various statistical measures.

Case A: Binary Classification of Diabetic Retinopathy with 1200 instances.

Machine Learning Model	**Accuracy**
Support Vector Machine	0.6634867
Random Forest	0.6657898
k-Nearest Neighbor	0.5176392
Adaboost	0.6621927
Artificial NN	0.6500546
Naive - Bayes	0.6482322
Linear Discriminant Analysis	0.6427890

Table 2: Binary Classification of Diabetic Retinopathy with 1200 instances.

Now refining these results by PCA(6 features generated):

Machine Learning Model	**New Accuracy**	**Previous Accuracy**	**Improvement**
Support Vector Machine	0.6623966	0.6634867	-0.0010901
Random Forest	0.6562298	0.6657898	-0.0095600

k-Nearest Neighbor	0.6101855	0.5176392	-0.0925463
Adaboost	0.6604919	0.6621927	-0.0017008
Artificial NN	0.6360106	0.6500546	-0.0140440
Naive - Bayes	0.6496172	0.6482322	0.0013849
Linear Discriminant Analysis	0.6519376	0.6427890	0.0091486

Table 3: Binary Classification of Diabetic Retinopathy with 1200 instances with PCA features.

Again trying to increase results by PCA(6 generated) + Our previous features:

Machine Learning Model	**New Accuracy**	**Previous Accuracy**	**Improvement**
Support Vector Machine	0.6642451	0.6623966	0.0018485
Random Forest	0.6737415	0.6562298	0.0175116
k-Nearest Neighbor	0.5124119	0.6101855	-0.0977736
Adaboost	0.6548930	0.6604919	-0.0055989
Artificial NN	0.6550138	0.6360106	0.0190033
Naive - Bayes	0.6365994	0.6496172	-0.0130177
Linear Discriminant Analysis	0.6432729	0.6519376	-0.0086647

Table 4: Binary Classification of Diabetic Retinopathy with 1200 instances and PCA features+ normal features.

Case B: Binary Classification of Macular Edema with 400 instances

Machine Learning Model	**Accuracy**
Support Vector Machine	0.7249993
Random Forest	0.7306538
k-Nearest Neighbor	0.5652262
Adaboost	0.6677390
Artificial NN	0.7218929
Naive - Bayes	0.7220698
Linear Discriminant Analysis	0.7312409

Now refining these results by PCA:

Machine Learning Model	**New Accuracy**	**Previous Accuracy**	**Improvement**
Support Vector Machine	0.7435463	0.7249993	-0.0010901
Random Forest	0.7061048	0.7306538	-0.0095600
k-Nearest Neighbor	0.6958272	0.5652262	-0.0925463
Adaboost	0.6981096	0.6677390	-0.0017008
Artificial NN	0.6706618	0.7218929	-0.0140440
Naive - Bayes	0.7216177	0.7220698	0.0013849
Linear Discriminant Analysis	0.7209671	0.7312409	0.0091486

Again, trying to increase precision by PCA(6 generated) + Our previous features estimation:

Machine Learning Model	**New Accuracy**	**Previous Accuracy**	**Improvement**
Support Vector Machine	0.7291922	0.7435463	-0.0143541
Random Forest	0.7302795	0.7061048	0.0241747
k-Nearest Neighbor	0.5659159	0.6958272	-0.0977736
Adaboost	0.7071550	0.6981096	0.0090455
Artificial NN	0.7333688	0.6706618	0.0627070
Naive - Bayes	0.7087025	0.7216177	-0.0129152
Linear Discriminant Analysis	0.7277994	0.7209671	0.0068323

Case C: Macular Edema multi classification for 1200 instances.

Accuracy under this case was 0.81 by random forests classifier with all 6 features included.

Now, under a special case as there is a correlation between FD and entropy. Entropy was removed and accuracy on the same was found to be 0.81.

5. CONCLUSIONS

Our image processing techniques have been very consistent. We have been successful in detecting blood vessels , microaneurysms and exudates. Results of extraction of blood vessels are found to be better than most of other works. A binary classifier system has been designed for diabetic retinopathy retinal defect has been developed and tested. This system provides an early warning of diabetic retinopathy abnormalities for diabetic patients. Extraction of haemorrhages have a lower accuracy. Microaneurysms are most important factor With correlation matrix we have been able to find that fractal dimensions and entropy have a positive correlation. This makes us free to drop one of these features without having much impact on accuracy.

We have tried our data on different models. The best accuracy achieved is for multiclass classification for macular edema with Random Forests Classifier using 1200 data points from MESSIDOR database.

6. References

1. Joshi, Shilpa, and P. T. Karule. "Retinal blood vessel segmentation." International Journal of Engineering and Innovative Technology (IJEIT) 1.3 (2012): 175-178.
2. Jaafar, Hussain F., Asoke K. Nandi, and Waleed Al-Nuaimy. "Automated detection of exudates in retinal images using a split-and-merge algorithm." Signal Processing Conference, 2010 18th European. IEEE, 2010.
3. Tripathi, Shraddha, et al. "Automatic detection of exudates in retinal fundus images using differential morphological profile." International Journal of Engineering and Technology 5.3 (2013): 2024-2029.
4. Decencière, Etienne, Xiwei Zhang, Guy Cazuguel, Bruno Lay, Béatrice Cochener, Caroline Trone, Philippe Gain, Richard Ordonez, Pascale Massin, Ali Erginay, Béatrice Charton, & Jean-Claude Klein. "FEEDBACK ON A PUBLICLY DISTRIBUTED IMAGE DATABASE: THE MESSIDOR DATABASE." Image Analysis & Stereology [Online], 33.3 (2014): 231-234. Web. 1 May. 2017

Tools and Technologies

1. OpenCV for Python, MATLAB: Used for Image Processing
2. R (packages- knitr, ggplot2, GGally, reshape2, e1071, randomForest, nnet, ROCR, adabag, class, MASS, caret), Python (Scikit-learn): Used for data analysis